Synthetic Data-Driven Approach for Missing Nut and Bolt Classification in Flange Joints

Frankly Toro[a], Hassane Trigui[b], Yazeed Alnumay[c], Siddharth Mishra[d] and Sahejad Patel[e]
Aramco, Thuwal, Saudi Arabia

Keywords: Asset Integrity, Flange Joints, Missing Bolt/Nut, Missing Nut, Multi-View CNN, Synthetic Data, Domain Adaptation, Image Classification, Grad-CAM.

Abstract: Inspection of bolted flange joints is a routine procedure typically done manually in process-based industries. However, this is a time-consuming task since there are many flanges in a typical operational facility. We present a computer vision-based tool that can be integrated into other systems to enable automated inspection of these flanges. We propose a multi-view image classification architecture for detecting a missing bolt or nut in a flange joint image. To guide the training process, a synthetic dataset with 60,000 image pairs was created to simulate realistic environmental conditions of flange joints. To demonstrate the effectiveness of our approach, an additional real-world dataset of 1,080 flange joint image pairs was manually collected. The proposed approach achieved remarkable performance in classifying missing bolt instances with an accuracy of 95.28% and 95.14% for missing nut instances.

1 INTRODUCTION

Flanges are commonly found in the energy industry to connect joints of pipelines with piping or plant equipment (Xue et al., 2019). These flanges are typically bolted together according to relevant standards to ensure the safe and reliable operation of the facilities. Fluctuations in thermodynamic parameters, pressure shocks, process upset, or other environmental phenomena can potentially disrupt the integrity of the flange joints, causing leaks and possibly leading to catastrophic disasters (Saad et al., 2022). To mitigate this, engineering departments develop inspection and maintenance protocols that govern the operation and maintenance of these flanges. These typically include periodic visual surveillance of flanges and taking corrective actions as needed.

One of the most critical components, particularly noted by maintenance personnel during an inspection, are the bolts and nuts, as most common flange anomalies are attributed to their dysfunction. Appropriate bolt torque is essential, as inaccurate bolt forces can lead to failure in the sealing of flange faces, causing leaks (Zhang et al., 2015). Typical bolt and nut related anomalies include: missing bolts/nuts, loose bolts/nuts, short bolting, and long bolting (ASME, 2019). These anomalies are typical after a major turnaround and inspection (T&I), where flanges are completely opened and maintained, wherein bolts or nuts are either missed or incorrectly installed. However, manually monitoring and inspecting flanges is time-consuming, considering the large number of flanges in a typical operational facility. As such, there is a need for an automated or more efficient inspection method for ensuring the complete

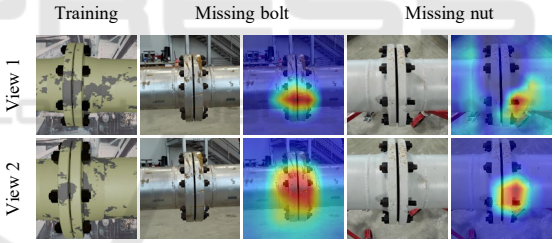

Figure 1: **Sample Results.** Our model uses two images of a flange from different perspectives to determine if a bolt or nut is missing. The model is trained on synthetically generated data. A real flange sample for each anomaly type is shown with two views, and GradCAM visualizes the model's focus on the anomaly.

[a] https://orcid.org/0000-0003-2379-7019
[b] https://orcid.org/0009-0002-5487-6326
[c] https://orcid.org/0000-0002-2475-8719
[d] https://orcid.org/0009-0002-8026-0242
[e] https://orcid.org/0000-0002-3824-9763

Toro, F., Trigui, H., Alnumay, Y., Mishra, S. and Patel, S.
Synthetic Data-Driven Approach for Missing Nut and Bolt Classification in Flange Joints.
DOI: 10.5220/0012271500003660

In *Proceedings of the 19th International Joint Conference on Computer Vision, Imaging and Computer Graphics Theory and Applications (VISIGRAPP 2024) - Volume 2: VISAPP*, pages 301-308
ISBN: 978-989-758-679-8; ISSN: 2184-4321

assembly of flanges with no missing parts to achieve the required integrity and process safety of flanges.

With the advancement of digitalization and Industrial Revolution (IR) 4.0, the oil and gas (O&G) industry is also going through a digital transformation effort (Wanasinghe et al., 2021). Accordingly, we propose a tool for automated visual inspection of flanges and define a computer vision-based pipeline that allows detecting anomalies on flange images, such as missing bolts and missing nuts from varied viewpoints. The scope of this paper is specifically targeted toward detecting a missing bolt or nut, as it serves as the first sanity check for flange integrity and its successful assembly. Due to the scarcity of real-world images, our method focuses on developing a robust model that can generalize well with real-world data while being trained on generated synthetic flange image data.

The generation of synthetic data using 3D modeling software was focused on creating a balanced dataset of representative flange images by randomly augmenting flange and scene conditions from various viewpoints. We artificially augmented 60,000 image pairs of training data using multiple spatial and pixel augmentations to train our proposed multi-view architecture. We validate the performance of the proposed method on real-world flanges with varying diameters: 8, 16, and 20 inches.

Our paper brings forth three major contributions: i) We introduce a 3D model for simulating flanges that can render images at various orientations, lighting, and spatial conditions. ii) We propose a multi-view image classification architecture for identifying a missing bolt or nut in a flange joint image. iii) We create a real-world dataset with 1,080 pairs of flange images divided into three balanced classes (healthy, missing nut, and missing bolt) manually captured and labeled for the test dataset.

2 RELATED WORK

The flange maintenance and integrity surveying process involves various inspection tasks. These inspections mostly revolve around bolt and nut integrity, as they are critical elements that hold the flange faces together with appropriate forces.

Contact-based solutions are typically used for bolt looseness detection (Nikravesh and Goudarzi, 2017; Wang et al., 2013) and include direct measurements using devices, such as strain gauges, or indirect methods of looseness detection, such as measuring vibrations and ultrasonic-based methods. These traditional techniques require manual operation and direct contact with the bolts. Therefore, they are costly and impractical for elevated and hard-to-reach flanges.

In addition to contact-based methods, academic research has leveraged computer vision algorithms for analyzing bolt tightness through bolt rotation detection. The framework of these methods can be generally classified into two main categories: classical computer vision and deep learning (DL). These solutions often aim to detect and quantify changes in the rotational orientation of bolts over time. The classical approaches (Park et al., 2015; Cha et al., 2016; Hongjian et al., 2015) perform perspective transforms to align the bolts, followed by a Hough transform line detection algorithm to detect rotations in the hexagonal screw heads.

On the other hand, while deep learning approaches still seek to assess the rotational movements of bolt heads over time, they employ a range of distinct techniques to achieve this goal. (Wang et al., 2019) uses handwritten digits on the bolts to detect and adjust for rotations by training on the MNIST digits dataset (Deng, 2012). Additionally, DBSCAN is used on the detected bolts to detect rotations. (Zhao et al., 2019) uses Single Shot MultiBox Detectors to infer rotations. Finally, (Sun et al., 2022) uses two colored markers on the bolt and the YOLOv5 object detection network to determine the bolt rotation.

These computer vision methods rely on rotation to measure bolt tightness but require a secure baseline image, which is often unavailable. In addition, frontal images of flanges are required, which can be more difficult to obtain than side images, particularly for elevated flanges.

Previous models for detecting missing bolts have been developed (Alnumay et al., 2022). However, their training set lacked diversity in flange types and was relatively small. Additionally, these models relied on a basic architecture, which restricted their performance. As a result, these models achieved higher testing accuracies only when tested on real images that closely matched the characteristics seen during training with a single model backbone. Furthermore, it is important to note that the real testing dataset used in their experiments was limited, comprising only 36 images. Consequently, when tested on our extensive real-image test dataset, these models demonstrated reduced classification accuracies, averaging around 65%.

In this paper, we tackle the fundamental problem of detecting a missing bolt or nut, as they are the first step towards a successful flange inspection. Unlike most previous work, our method requires no prior intervention or markings on the flange. Additionally, it is robust to various types of bolts and nuts.

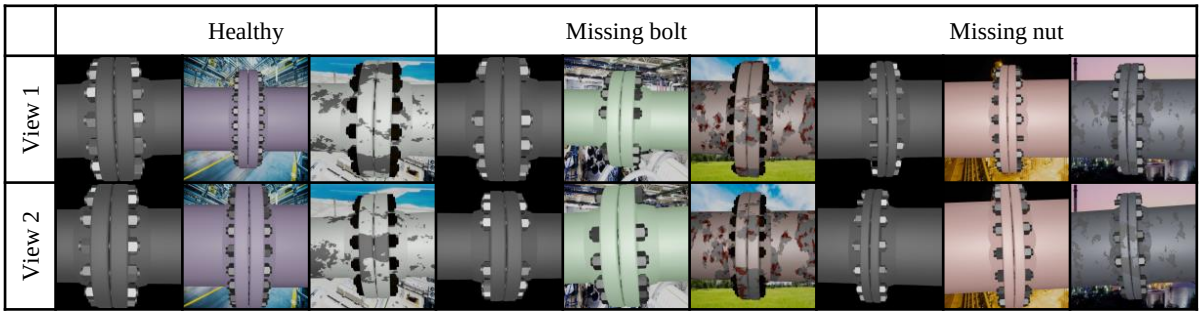

Figure 2: **Synthetic Image Samples.** Pairs of images representing each of the three classes within our training dataset. The synthetic images, generated using Blender, exhibit variations in size, paint, rust, and camera perspective, corresponding to different dataset versions. Here, we present three distinct dataset versions.

3 FLANGE ANOMALY DETECTION METHOD

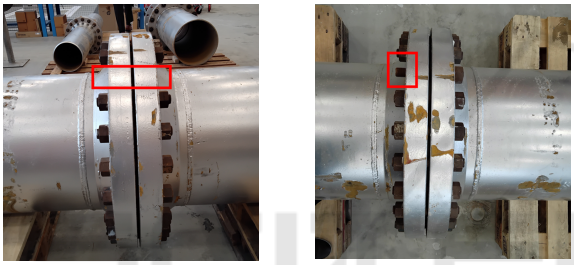

(a) Missing bolt (b) Missing nut

Figure 3: Anomaly examples.

The model development process is divided into two stages. First, generate synthetic training data. Second, fine-tuning an image classification network pretrained on ImageNet (Deng et al., 2009). The initial stage generates synthetic flanges from 3D models to produce surrogate training data. The second component outlines the Deep Learning (DL) Network architecture for image classification using single and multiple flange views as inputs. The goal of this network is to identify whether a given image or a pair of images of a flange joint has a missing nut or bolt. Examples of such anomalies are shown in Figure 3

3.1 Synthetic Data Generation

Training an effective deep learning model typically requires large labeled datasets. However, obtaining sufficient images of flanges with varying sizes, materials, environments, and anomaly locations is labor-intensive. Therefore, our method relies on generating labeled synthetic images to create our training set.

Our synthetic images were generated using the open-source 3D modeling and animation software Blender (Blender, 2018). We designed a 3D model of a flange joint that enables us to control some basic visual characteristics, such as standardized dimensions following the ASME 16.5 specifications (ASME, 2020), paint color, background, rust, bolt, and nut color.

Blender's flexibility enables the generation of various flange joints by adjusting physical parameters and camera settings and simulating ground truth values to train supervised deep learning models.

We developed a Blender script to randomly sample parameters for the camera, flange dimensions, and anomaly locations. The script renders pairs of images for each flange and records the ground-truth class label. A sample of this dataset is shown in Figure 2. The resulting synthetic dataset contains 60,000 image pairs, with 20,000 pairs for each of the three classes: healthy, missing bolt, and missing nut. The synthetic data was split into a proportion of 60/20/20 for training/validation/testing.

The diversity and realism of synthetic datasets considerably impact model performance. In our initial models, we generated basic and untextured flange renders without background. These models produced high-accuracy results when applied to synthetic data. However, the feature distributions between synthetic and real images differed significantly, limiting the use of the models on real images. Consequently, our initial models produced nearly random results when tested on real images. To address this disparity, we adopted an iterative approach, refining our synthetic dataset based on observed characteristics in real images (see Figure 2). This strategy continued until we achieved the satisfactory results presented in section 4.

The synthetic data was generated using all flange sizes between 3–24 inches and pressure classes of 150 and 300 pounds, as described in the ASME 16.5 standard. We uniformly sampled the flange size and class

from the finite set of sizes and classes. We added camera perturbations to the synthetic image pairs to closely emulate real images because it is unrealistic to expect the user to dependably capture the flange at specified viewpoints and distances in both views. In addition, we constrained these perturbations so that the bolts and nuts from both sides of the joint flange were always visible in the image. Detailed attribute variations are described in Table 1.

Table 1: **Synthetic Data Camera Attributes.** $\mathcal{N}(\mu, \sigma^2)$ denotes a normal distribution with mean μ and standard deviation σ. $\mathcal{U}(a, b)$ denotes a uniform distribution on the range $[a, b]$. These attributes are sampled independently, even for different views of the same image pair. The sampled values are clamped if they exceed the specified range.

Attribute	Distribution	Range
Camera pan	$\mathcal{N}(0, 3^2)$	$[-5°, +5°]$
Camera tilt	$\mathcal{N}(0, 1^2)$	$[-2°, +2°]$
Camera roll	$\mathcal{N}(0, 1^2)$	$[-2°, +2°]$
Zoom percentage	$\mathcal{U}(-15, +15)$	$[-15, +15]$
2-view angle difference	$45 + \mathcal{N}(0, 10^2)$	$[20°, 70°]$

3.2 Model Architecture

We developed two main model architectures, single-view, and multi-view, which take one or two images, respectively. We tested multiple state-of-the-art backbone architectures for our single- and multi-view approaches to classify a missing nut or bolt. These include ViT (Dosovitskiy et al., 2020), ConvNeXt (Liu et al., 2022), and SqueezeNet (Iandola et al., 2016). Additionally, for comparison purposes with (Alnumay et al., 2022), we tested a VGG-16 (Simonyan and Zisserman, 2015) backbone for the missing bolt model. For each architecture, two independent models were developed, one for missing bolt and the other for missing nut.

3.2.1 Single-View

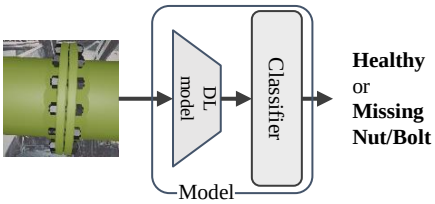

Figure 4: Single-view model architecture.

The single-view architecture, shown in Figure 4, is a standard image classification pipeline where we input a single image and output whether a flange is healthy or anomalous. We tested various CNN and transformer-based backbones.

3.2.2 Multi-View

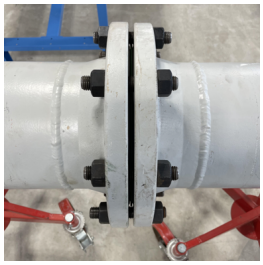

(a) Flange appears to have a missing bolt in the middle

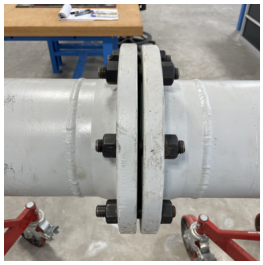

(b) Flange appears healthy after perspective change

Figure 5: **Perspective is Critical.** When observed from non-ideal viewpoints, a healthy flange may appear to be missing a nut or bolt due to center nuts and bolts being closer to the camera and lens distortions on nuts and bolts closer to the image's edge.

Our multi-view model architecture is inspired by (Su et al., 2015), where they used a multi-view CNN (MVCNN) to improve the 3D object recognition performance of CNNs by taking images from multiple angles. We hypothesized that this architecture could benefit our task, as we noticed that some perspectives can be deceiving, as illustrated in Figure 5. Additionally, MVCNN methods have improved performance compared to single-view methods alone in other industrial use cases (Tilgner et al., 2019; Shamsafar et al., 2023).

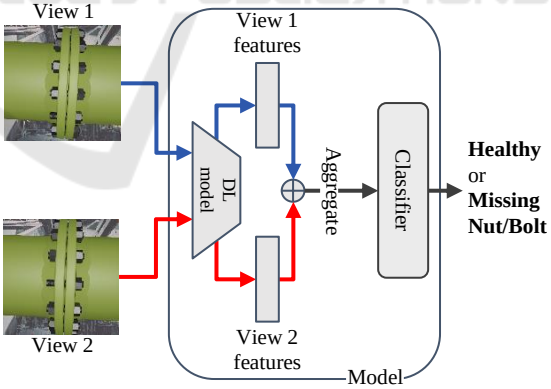

Figure 6: Multi-view model architecture.

Figure 6 summarizes the architecture of our multi-view model. It is similar to the single-view model in that it takes images of flanges and outputs a classification if they are healthy or anomalous. Again, two separate models were developed to identify a missing bolt or nut. However, this model takes two images of the same flange from different perspectives as inputs. It extracts features of each view from the same DL model. These features are then combined and passed

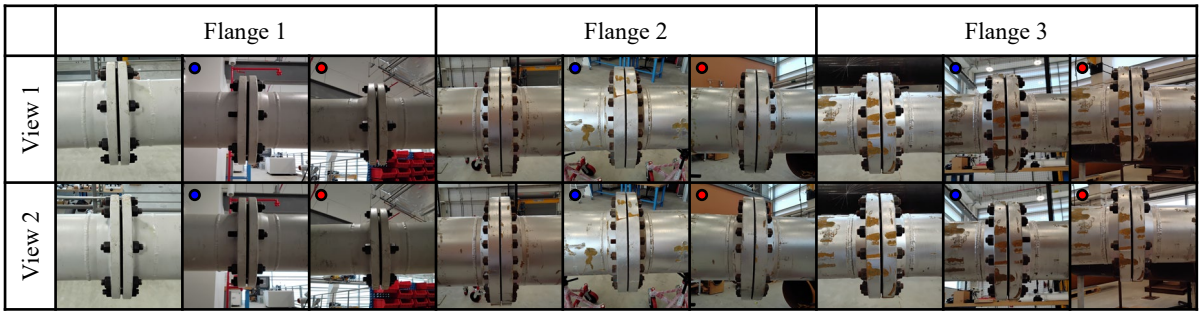

Figure 7: **Real Image Samples.** Sample image pairs from three real flanges that form our testing set. • indicates a missing nut, while • indicates a missing bolt. The perspectives and backgrounds were varied for all anomalies and flange combinations.

to the final classification network. We attempted to use various combination methods for the two feature vectors, such as taking the sum, concatenation, maximum, or adding an attention layer. The best aggregation method for missing nut was concatenating the feature vectors, and the best method for missing bolt was taking the mean of the two feature vectors. Similar to the single-view model, we experimented with multiple CNN and transformer-based backbones.

Our experimental setup used state-of-the-art deep convolutional neural network architectures pretrained on the ImageNet dataset. We fine-tuned these models for our specific tasks. We utilized the widely adopted Adam optimizer with a learning rate of 0.00008 and ReduceLROnPlateau with a factor of 10 to facilitate rapid convergence. The batch size was set to 16, and data augmentation techniques were applied to enhance the model's generalization capability, including photometric transformation such as random flips, sun flares, brightness, occlusions, and color jittering. The training was conducted on a high-performance computing cluster equipped with NVIDIA A100 GPUs, expediting convergence and significantly reducing training time. Our training pipeline was implemented in PyTorch 2.0, leveraging the CUDA toolkit for GPU acceleration. These hyperparameters and resources were selected by an extensive grid search and rigorous cross-validation to ensure the best performance on our specific tasks.

4 RESULTS AND ANALYSIS

In this section, we first describe our Real Test Dataset. Then, we provide the evaluation of our models in the proposed test dataset for missing nut or bolt. In addition, we use GradCAM (Selvaraju et al., 2017), an interpretability technique that highlights the important regions of an image used by a CNN to make a particular classification decision to explain these results qualitatively. Finally, we compare the performance of our method against the previous work (Alnumay et al., 2022) in the case of missing bolt.

4.1 Real Test Dataset

This lab-based dataset was manually collected using a tablet device equipped with an HD camera. It comprises images of three distinct flange joints, each associated with different pipe sizes: 8, 16, and 20 inches. Every image in the dataset was rigorously labeled according to our three classes: healthy, missing nut, and missing bolt. Importantly, we maintained a uniform number of images within each class, ensuring a balanced dataset.

To replicate real-world conditions, the flanges in our dataset exhibit environmental wear and tear. Additionally, controlled movement of the flanges was included during image capture to provide diverse yet natural backgrounds and lighting effects.

In the multi-view configuration, we captured 360 image pairs for each class, resulting in 1,080 image pairs, equivalent to 2,160 individual images. Figure 7 shows a subset of our real dataset as image pairs. In the single-view configuration, we exclusively used the first image from each pair. This decision was grounded in the assumption that the distribution between the two views remains identical, leaving the second image redundant for single-view analysis. Each image pair was captured from a different viewpoint by moving the tablet's camera around the flange. These viewpoint variations were randomly selected within a range of $\pm 20^{\circ}$ to emulate natural human movement during the capturing process.

4.2 Missing Nut

We started by evaluating the effectiveness of our two methods in identifying a missing nut on the Real Test Dataset. For this evaluation, we leveraged the synthetic dataset to fine-tune state-of-the-art backbones, such as ConvNeXt, ViT, and SqueezeNet. Table 2

summarizes the results.

The best results are obtained with the ConvNeXt backbone in both methods, single-view and multi-view. Our method's comparison shows that the multi-view approach consistently outperforms the single-view. In addition, the performance of our method is greatly improved with the synthetic data when using a multi-view approach as opposed to a single-view.

We observed that the multi-view method could reduce the gap between synthetic and real domains for the analyzed backbones to make inferences on real data while training only on synthetic images. Our best model reports an accuracy of 82.22% using the multi-view method, while the best single-view model only reports 66.81%.

To enhance the generalization capabilities of our multi-view model while mitigating overfitting on the Real Test Dataset, we applied the feature alignment technique AdaBN (Li et al., 2018). This approach further improved the accuracy to 95.14%.

Table 2: **Missing Nut Results.** Testing accuracies for missing nut detection, based on the Real Test Dataset. Multi-view increases the accuracy by 15% and by 28% when combined with AdaBN

Method	ConvNeXt	ViT	SqueezeNet
Single-View	**66.81**	62.81	57.36
Multi-View	**82.22**	76.39	72.92
Multiview + AdaBN	**95.14**	–	–

4.2.1 Qualitative Analysis

We tested our methods on real-world flanges (Real Test Dataset). Figure 8 shows classification samples as a visual confusion matrix. The model's areas of interest for correct classifications focus more on the whole flange for healthy flanges and the nuts for missing nut cases. The false positive probably occurred from other background flanges confusing the model, while the false negative can likely be attributed to a short bolt.

Overall, we observe a considerable difference in recall between our two methods for the healthy and missing nut classes. Our single-view method correctly predicts more healthy flanges than missing nut instances. However, while our multi-view approach successfully predicts almost every case of missing nut, it fails to identify more healthy flange cases.

4.3 Missing Bolt

We followed the same methodology as in subsection 4.2 to assess our two methods for identifying a missing bolt. Additionally, we compare our results to prior work (Alnumay et al., 2022). Table 3 summarizes the results.

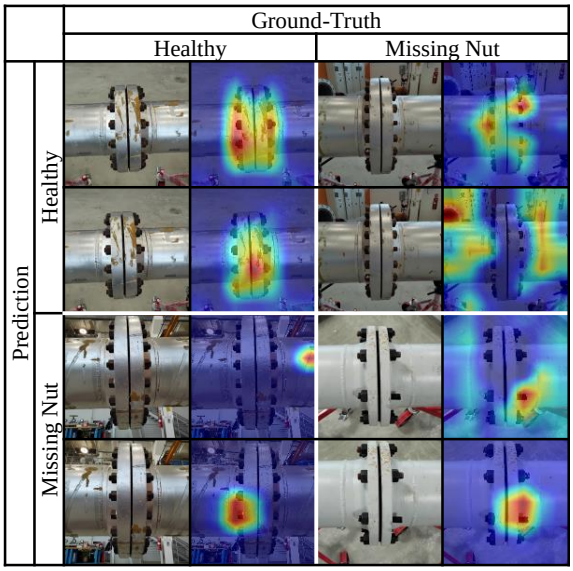

Figure 8: **Missing Nut Qualitative Results.** We show sample images of correct and incorrect classifications, using the multi-view method and ConvNeXt backbone, for missing nut as a visual confusion matrix. We use GradCAM's visualization capabilities to highlight the model's areas of interest used for classification.

4.3.1 Comparison Against Prior Work

The work of (Alnumay et al., 2022) collects its own real-world dataset. Their test set consists of 36 images, where 20 images belong to missing bolt instances of the same flange (8 inches) and 16 images of healthy flanges, where 68% of the cases are from the 8-inch flange. Due to the precise data imbalance and bias towards 8-inch flanges, we run their proposed model in our test set (see details in subsection 4.1) and perform a direct comparison.

Our model displays notable robustness when confronted with various pipe sizes, even in cases where the size is not explicitly provided as input, inferring the pipe size from flange to pipe ratio. Leveraging this unique ability, the model proficiently determines the number of bolts required for a specific flange type set forth by the relevant standards.

Overall, we observe that our best single-view model (ConvNeXt) outperforms the comparable model of (Alnumay et al., 2022) by 9%. Likewise, our best multi-view model (ViT) outperforms (Alnumay et al., 2022) model by 29%. This suggests that our proposed multi-view model has a better generalization capability than prior work.

4.3.2 Real Dataset Evaluation

In contrast to Table 2, different backbone models produce the best results for each method. In particular, ViT succeeds in multi-view, whereas ConvNeXt stands out in single-view. Additionally, our multi-view approach consistently exceeded the performance of single-view models, as previously seen in subsection 4.2. This outcome emphasizes the advantages of leveraging a multi-view method.

In general, our findings suggest that identifying a missing bolt is significantly easier than identifying a missing nut due to the salient visual cues present in the images. When identifying missing bolts, we observed three instances of missing items (2 nuts and 1 bolt) compared to only one instance of a missing item (one nut) when identifying missing nuts. The analysis of the GradCAM results showed a significant difference in attention distribution. For missing bolts, attention was mainly on the flange and bolt-related elements, while for missing nuts, attention was more scattered. The multi-view method alone achieved the highest accuracy for missing bolts at 95.28% and for missing nuts at 82.22%. Our best single-view model for detecting a missing bolt has an accuracy of 75.28%. Additionally, by using feature alignment methodologies, we can increase the accuracy of missing nut identification to 95.14%.

Contrary to the promising results observed in Table 2, applying AdaBN to our multiview model for identifying missing bolts resulted in a 5% decrease in accuracy, significantly compromising the model's generalization capabilities.

Table 3: **Missing Bolt Results.** Testing accuracies for missing bolt detection, based on the Real Test Dataset. Multi-view increases the accuracy by 20%.
* VGG model from (Alnumay et al., 2022) tested on our Real Test Dataset.

Method	ConvNeXt	ViT	SqueezeNet	VGG*
Single-View	**75.28**	73.61	55.14	65.83
Multi-View	90.14	**95.28**	91.11	–
Multiview + AdaBN	–	90.28	–	–

4.3.3 Qualitative Analysis

We tested our methods on real-world flanges (Real Test Dataset). Figure 9 shows classification samples as a visual confusion matrix. The model's areas of interest for correct classifications focus more on bolts for healthy flanges and the specific regions where missing bolt cases happen. The false positive case likely resulted from background objects in the top image, while there is no clear indicator for the cause of the false negative. However, it is noted that

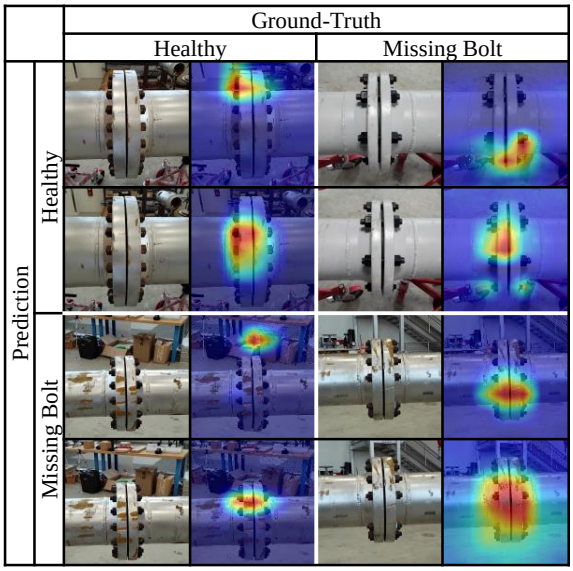

Figure 9: **Missing Bolt Qualitative Results.** We show sample images of correct and incorrect classifications, using the multi-view method and ConvNeXt backbone, for missing bolt as a visual confusion matrix. We use GradCAM's visualization capabilities to highlight the model's areas of interest used for classification.

when images with similar viewpoints are provided to the network, the model may be confused and focus on areas that appear to have missing bolts.

Overall, we observe a considerable difference in recall between our two methods for the healthy and missing bolt classes. Our single-view method correctly predicts more healthy flanges than missing nut instances. However, our multi-view approach successfully reduces the number of misclassified instances for both healthy and anomalous cases.

5 CONCLUSION AND FUTURE WORK

In this paper, we present a multi-view image classification approach based on computer vision for detecting a missing nut or bolt in a flange joint image. This was achieved using CNN and transformer-based networks that were exclusively trained on synthetic image data and augmented with varying parameters encountered in real scenarios. The model demonstrated its efficacy when tested on a real-world dataset, illustrating robust performances in most scenarios.

In future work, we aim to enhance material and texture modeling and illumination techniques for synthetic images, benchmark the number of views, and evaluate the model's performance in detecting multi-

ple missing nuts or bolts, short/long and loose bolts using our two-step methodology. We will also explore domain adaptation techniques to reduce the gap between the source and target domains.

ACKNOWLEDGEMENTS

This publication is based on work supported by the Research & Development Center of Saudi Aramco. We also acknowledge the King Abdullah University of Science and Technology (KAUST) for providing computational resources.

REFERENCES

Alnumay, Y., Alrasheed, A. J., Trigui, H., et al. (2022). Synthetic data generation for machine learning applications in the energy industry. In *ADIPEC*, page D021S052R003. SPE.

ASME (2019). ASME PCC-1 pressure boundary bolted flange joint assembly.

ASME (2020). ASME 16.5B pipe flanges and flanged fittings: Nps 1/2 through nps 24, metric/inch standard.

Blender (2018). *Blender - a 3D modelling and rendering package*. Blender Foundation, Stichting Blender Foundation, Amsterdam.

Cha, Y.-J., You, K., and Choi, W. (2016). Vision-based detection of loosened bolts using the hough transform and support vector machines. *Automation in Construction*, 71:181–188.

Deng, J., Dong, W., Socher, et al. (2009). ImageNet: A Large-Scale Hierarchical Image Database. In *CVPR09*.

Deng, L. (2012). The mnist database of handwritten digit images for machine learning research. *IEEE signal processing magazine*, 29(6):141–142.

Dosovitskiy, A., Beyer, L., Kolesnikov, A., et al. (2020). An image is worth 16x16 words: Transformers for image recognition at scale. *arXiv:2010.11929*.

Hongjian, Z., Ping, H., and Xudong, Y. (2015). Fault detection of train center plate bolts loss using modified lbp and optimization algorithm. *The Open Automation and Control Systems Journal*, 7(1).

Iandola, F. N., Han, S., Moskewicz, et al. (2016). Squeezenet: Alexnet-level accuracy with 50x fewer parameters and less than 0.5 mb model size. *arXiv preprint arXiv:1602.07360*.

Li, Y., Wang, N., Shi, J., et al. (2018). Adaptive batch normalization for practical domain adaptation. *Pattern Recognition*, 80:109–117.

Liu, Z., Mao, H., Wu, C.-Y., et al. (2022). A convnet for the 2020s. In *Proceedings of the IEEE/CVF CVPR*, pages 11976–11986.

Nikravesh, S. M. Y. and Goudarzi, M. (2017). A review paper on looseness detection methods in bolted structures. *Latin American Journal of Solids and Structures*, 14:2153–2176.

Park, J.-H., Huynh, T.-C., Choi, S.-H., et al. (2015). Vision-based technique for bolt-loosening detection in wind turbine tower. *Wind Struct*, 21(6):709–726.

Saad, S., Ekhwan, A., and Al-Idrus, S. M. H. (2022). Bolted Flange Joint Integrity Digitalization Programme for Sustainable Flange Leak Free Operation. *Offshore Technology Conference Asia*, Day 4 Fri, March 25, 2022:D041S041R003.

Selvaraju, R. R., Cogswell, M., Das, A., et al. (2017). Grad-cam: Visual explanations from deep networks via gradient-based localization. In *Proceedings of the IEEE ICCV*, pages 618–626.

Shamsafar, F., Jaiswal, S., Kelkel, B., et al. (2023). Leveraging multi-view data for improved detection performance: An industrial use case. In *Proceedings of the IEEE/CVF CVPR Workshops*, pages 4463–4470.

Simonyan, K. and Zisserman, A. (2015). Very deep convolutional networks for large-scale image recognition.

Su, H., Maji, S., Kalogerakis, E., and Learned-Miller, E. (2015). Multi-view convolutional neural networks for 3d shape recognition. In *Proceedings of the IEEE ICCV*.

Sun, Y., Li, M., Dong, R., Chen, W., and Jiang, D. (2022). Vision-based detection of bolt loosening using yolov5. *Sensors*, 22(14):5184.

Tilgner, S., Wagner, D., Kalischewski, K., et al. (2019). Multi-view fusion neural network with application in the manufacturing industry. In *2019 IEEE ISCAS*, pages 1–5.

Wanasinghe, T., Trinh, T., Nguyen, T., et al. (2021). Human centric digital transformation and operator 4.0 for the oil and gas industry. *IEEE Access*, PP:1–1.

Wang, C., Wang, N., Ho, S.-C., et al. (2019). Design of a new vision-based method for the bolts looseness detection in flange connections. *IEEE Transactions on Industrial Electronics*, 67(2):1366–1375.

Wang, T., Song, G., Liu, S., Li, Y., and Xiao, H. (2013). Review of bolted connection monitoring. *International Journal of Distributed Sensor Networks*, 9(12):871213.

Xue, J., Chen, X., Fan, Z., et al. (2019). Effect of internal pressure on gasket stress and leakage rate of bolted flanged joint during the long term service at high temperature. In *Pressure Vessels and Piping Conference*, volume 58936, page V002T02A031. ASME.

Zhang, L., Liu, Y., Sun, J., et al. (2015). Research on the assembly pattern of mmc bolted flange joint. *Procedia Engineering*, 130:193–203.

Zhao, X., Zhang, Y., and Wang, N. (2019). Bolt loosening angle detection technology using deep learning. *Structural Control and Health Monitoring*, 26(1):e2292.